

High definition ultrasound imaging of the individual elements of the brachial plexus above the clavicle

Manoj Kumar Karmakar , Jatuporn Pakpirom, Banchobporn Songthamwat, Pornpatra Areeruk

► Additional material is published online only. To view please visit the journal online (<http://dx.doi.org/10.1136/rapm-2019-101089>).

Correspondence to

Professor Manoj Kumar Karmakar, Department of Anaesthesia and Intensive Care, Chinese University of Hong Kong Faculty of Medicine, New Territories, Shatin, Hong Kong; karmakar@cuhk.edu.hk

Received 23 October 2019
Revised 21 January 2020
Accepted 26 January 2020
Published Online First
25 February 2020

ABSTRACT

Background and objectives Ultrasonography of the brachial plexus (BP) has been described but there are limited data on visualization of the T1 ventral ramus and the inferior trunk. This prospective observational study aimed to evaluate a high definition ultrasound imaging technique to systematically identify the individual elements of the BP above the clavicle.

Methods Five healthy young volunteers underwent high definition ultrasound imaging of the BP above the clavicle. The ultrasound scan sequence (transverse oblique scan) commenced at the supraclavicular fossa after which the transducer was slowly swept cranially to the upper part of the interscalene groove and then in the reverse direction to the supraclavicular fossa. The unique sonomorphology of the C7 transverse process was used as the key anatomic landmark to identify the individual elements of the BP in the recorded sonograms.

Results The neural elements of the BP that were identified in all volunteers included the ventral rami of C5–T1, the three trunks, divisions of the superior trunk, and formation of the inferior trunk (C8–T1). The C6 ventral ramus exhibited echogenic internal septation with a split (bifid) appearance in four of the five volunteers. In three of the four volunteers with a bifid C6 ventral ramus, the C7 ventral ramus was also bifid.

Conclusion We have demonstrated that it is feasible to accurately identify majority of the main components of the BP above the clavicle, including the T1 ventral ramus and the formation of the inferior trunk, using high definition ultrasound imaging.

Trial registration number ChiCTR1900021749.

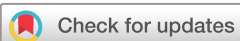
INTRODUCTION

Interscalene brachial plexus block (BPB) is frequently used for anesthesia or analgesia during shoulder surgery, and today it is widely performed using ultrasound guidance.¹ During an ultrasound guided (USG) interscalene BPB, the neural elements of the brachial plexus (BP) are imaged in the transverse (axial) oblique plane¹ and in the upper part of the “interscalene groove.”^{1 2} The neural elements are visualized as three round to oval hypoechoic structure,^{1–3} each surrounded by a thin hyperechoic rim³ and sandwiched between the scalenus anterior and scalenus medius muscles.^{1–3} A recent report⁴ drew attention to the lack of consensus on the identity of the hypoechoic nerves in a transverse oblique sonogram of the interscalene groove.⁴ They have been described variably by different authors as the “roots,”^{5–8} “nerve roots,”⁹

“brachial plexus root,”^{10 11} “ventral ramus,”^{12 13} “BP elements or components,”^{2 8} “trunks,”^{1 14} or even as the “nerve roots and trunks”² of the BP. Others have also labeled all five elements of the BP (C5–T1) in a single sonogram of the neck.^{6 7 10} As a result, there are several reports highlighting the possible “mislabeling” or “misidentification” of the nerves within the interscalene groove in published images.^{10 15} Moreover, Franco and Williams⁴ have recently demonstrated in cadavers that the “stop-light sign,”⁴ that is often used to describe the three hypoechoic elements of the BP within the interscalene groove,^{1–3} is made up of only two roots of the BP (C5 and C6) and there is no contribution from the C7 root. Franco and Williams’s⁴ finding may have implication for safety during USG interscalene BPB, particularly inadvertent intraneural injection of the C6 root of the BP, if the operator is unable to accurately identify the splitting of the C6 root.⁴ Furthermore, recently selective “anterior suprascapular nerve block”¹⁶ and “superior (upper) trunk block”¹⁷ have been described as alternatives to interscalene BPB for shoulder surgery. Therefore, for safety and efficacy, it is desirable that every practitioner of USG interscalene BPB is able to accurately identify the individual elements of the BP above the clavicle. Currently, there are numerous reports on ultrasound imaging of the BP,^{2 3 7 9 11 12} and how to accurately identify the ventral rami of C5–C7,^{3 11 12 18 19} but there is a paucity of data on ultrasound imaging of the ventral rami of C8 and T1.^{10 11 18 19} There are also reports suggesting that ultrasound imaging of the T1 ventral ramus is not possible.^{5 9} The aim of this study was to evaluate a high definition ultrasound imaging technique, using scan planes that are typically used during USG BPB,¹² to systematically identify the individual elements of the BP above the clavicle including the ventral rami of C8 and T1 and formation of the inferior trunk.

METHODS

Five young adult volunteers who gave written informed consent to undergo unilateral (right sided) ultrasound examination of the BP were included. Volunteers who were obese, had a short neck or had previous surgery on the neck were excluded. All ultrasound scans were performed by a single investigator (MKK) using a high definition Philips iU22 ultrasound system (Philips Healthcare, Andover, Massachusetts) with a high-frequency (L12-5 MHz, 50 mm footprint) linear array transducer. Volunteers were positioned supine, with the arm in the



© American Society of Regional Anesthesia & Pain Medicine 2020. No commercial re-use. See rights and permissions. Published by BMJ.

To cite: Karmakar MK, Pakpirom J, Songthamwat B, et al. *Reg Anesth Pain Med* 2020;**45**:344–350.

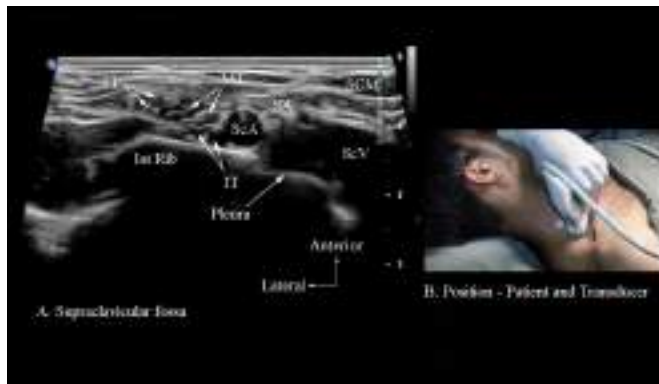


Figure 1 (A) Transverse oblique sonogram of the brachial plexus at the supraclavicular fossa. The trunks and division of the brachial plexus are visualized as a cluster of nerves on the posterolateral aspect of the subclavian artery. (B) Position of patient and ultrasound transducer during the scan. IT, inferior (lower) trunk; MT, middle trunk; SA, scalenus anterior; ScA, subclavian artery; SCM, sternocleidomastoid muscle; ScV, subclavian vein; ST, superior (upper) trunk.

neutral position, neck slightly extended and the head turned slightly to the contralateral side, for the ultrasound scan. The ultrasound image was optimized by selecting the most appropriate frequency, depth, focus, gray scale map, gain (time gain compensation) and dynamic range settings. “Write zoom” was also used because it produces greater line density, faster screen refresh rate, and an overall improved resolution of the “area of interest.” Optimized ultrasound images of the individual ventral ramus (roots), trunks, and divisions of the BP were captured digitally, on to the hard disc of the ultrasound system, as a short video loop (6 s each) for review.

The ultrasound scan sequence

The ultrasound scan was performed sequentially over seven contiguous sites (figures 1–7) starting from the base of the neck (supraclavicular fossa) to the upper part of the interscalene groove and then in the reverse direction to the supraclavicular

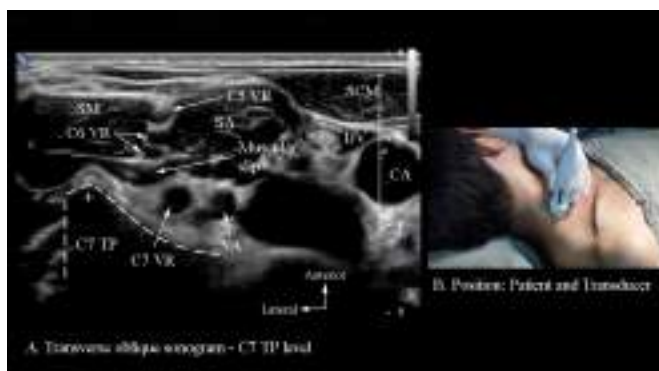


Figure 2 (A) Transverse oblique sonogram of the neck at the level of the C7 transverse process. Note the C7 transverse process has only one tubercle (ie, the posterior tubercle). The anterior tubercle is either absent or rudimentary. Note the C6 ventral ramus is split (bifid) and there is a muscular slip that connects the scalenus anterior and scalenus medius muscle and separates the C6 and C7 ventral rami. (B) Position of patient and ultrasound transducer during the scan. CA, carotid artery; IJV, internal jugular vein; SA, scalenus anterior; SCM, sternocleidomastoid muscle; SM, scalenus medius muscle; TP, transverse process; VA, vertebral artery; VR, ventral ramus.

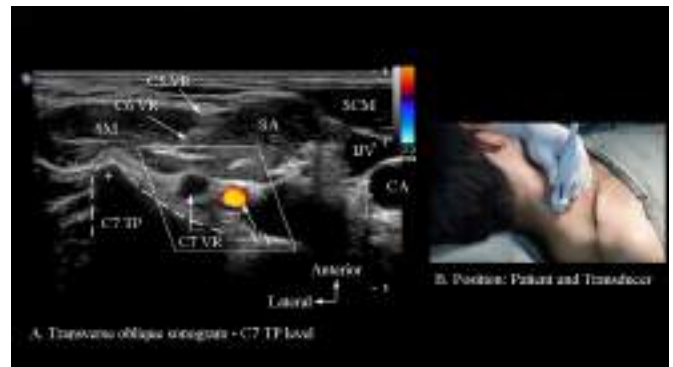


Figure 3 Figure 3(A) Color Doppler sonogram of the neck at the level of the C7 transverse process. Note the C7 ventral ramus is located lateral to the vertebral artery and anterior to the C7 transverse process. (B) Position of patient and ultrasound transducer during the scan. CA, carotid artery; IJV, internal jugular vein; SA, scalenus anterior muscle; SCM, sternocleidomastoid muscle; SM, scalenus medius muscle; TP, transverse process; VA, vertebral artery; VR, ventral ramus.

fossa. This was done to ensure consistency and to better define the contiguous anatomy of the BP nerves at the target sites. Liberal amount of ultrasound gel was applied to the skin for acoustic coupling and the ultrasound scan was commenced at the supraclavicular fossa. Once the ultrasound image was optimized, the transducer was slowly manipulated cranially with a sweeping motion, following the BP nerves, to the upper part of the interscalene groove and then slowly back down to the supraclavicular fossa. During the ultrasound scan, the orientation of the ultrasound transducer changed from being transverse oblique with a caudal angulation at the supraclavicular fossa (figure 1) to transverse (axial) oblique at the lateral aspect of the neck (figures 2–7) and then transverse oblique with a caudal angulation once again at the supraclavicular fossa (figure 1). The position and orientation of the ultrasound transducer at each location during the ultrasound scan sequence is illustrated in figures 1–9.

Ultrasound imaging of the BP above the clavicle is an extraforaminal examination^{3,9} and after the “cervical spinal nerves”

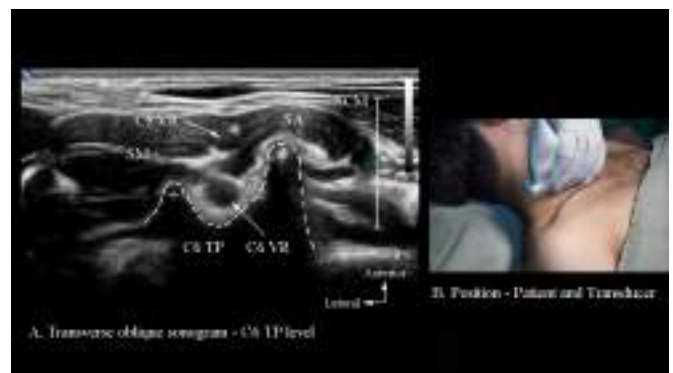


Figure 4 (A) Transverse oblique sonogram of the neck at the level of the C6 transverse process (TP). The outlines of the anterior (*) and posterior (+) tubercles of the TP have been highlighted in the sonogram. Note the prominent anterior tubercle and the hypoechoic C6 ventral ramus emerging between the two tubercles of the C6 TP. The smaller C5 ventral ramus is visualized cephalad to the C6 ventral ramus. (B) Position of patient and ultrasound transducer during the scan. SA, scalenus anterior muscle; SCM, sternocleidomastoid muscle; SM, scalenus medius muscle; VR, ventral ramus.



Figure 5 (A) Transverse oblique sonogram of the neck at the level of the C5 transverse process (TP). The outlines of the anterior (*) and posterior (+) tubercles of the TP have been highlighted in the sonogram. Note the hypoechoic C5 ventral ramus emerging between the two tubercles of the C5 TP. (B) Position of patient and ultrasound transducer during the scan. CA, carotid artery; DSN, dorsal scapular nerve; IJV, internal jugular vein; LTN, long thoracic nerve; SA, scalenus anterior muscle; SCM, sternocleidomastoid muscle; SM, scalenus medius muscle; VR, ventral ramus.

have emerged from the intervertebral foramen.³ Therefore, ultrasound imaging cannot depict the “cervical nerve roots” because they are located deep within the spinal canal and not amenable to ultrasound due to acoustic shadowing by bone.³ So in order to avoid confusion between the terms “root of the BP” with the “cervical nerve root,” we will henceforth refer to the “roots of the BP” as the “ventral ramus” in this report.

The ultrasound scan sequence included the following steps: *Step I:* the ultrasound transducer was placed directly cranial to the midpoint of the clavicle with its orientation marker directed laterally (outward). The aim was to visualize the subclavian artery on top of the first rib with the BP (trunks and division) appearing as a “cluster-of-grapes”¹⁴ on the posterolateral aspect of the subclavian artery (Figure 1, online supplementary digital content 1). In order to obtain the best possible view of the BP, the ultrasound transducer was also gently tilted caudally as described above (figure 1).^{2,8} *Step II:* the transducer was then

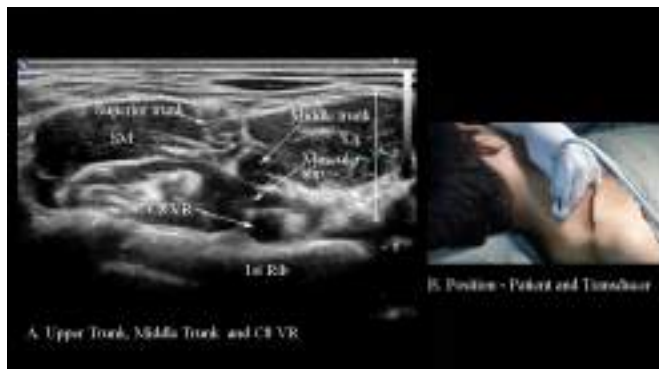


Figure 6 (A) Transverse oblique sonogram of the neck at the level where the superior trunk (C5–C6) is formed by fusion of the C5 and C6 ventral rami. Note the relationship of the middle trunk and C8 ventral ramus (deep and caudal) to the superior trunk. The C8 ventral ramus is also located on top of the T1 transverse process and first rib complex. Also note the muscular slip lying deep to the scalenus anterior muscle and passing between the middle trunk and C8 ventral rami. (B) Position of patient and ultrasound transducer during the scan. SA, scalenus anterior; SM, scalenus medius; VR, ventral ramus.



Figure 7 (A) Transverse oblique sonogram of the neck illustrating the divisions of the superior trunk. Note the “SPA arrangement” of the three divisions of the superior trunk, suprascapular nerve, posterior division and anterior division, from a lateral to medial direction. (B) Position of patient and ultrasound transducer during the scan. MT, medial trunk; SA, scalenus anterior muscle; ScA, subclavian artery; SM, scalenus medius muscle; SSN, suprascapular nerve; STa, anterior division of superior trunk; STp, posterior division of the superior trunk; VR, ventral ramus.

slowly manipulated cranially with a sweeping motion until the transverse process (TP) of C7 was identified (Fig. 2, online supplementary digital content 2). The TP of C7 is typically large, has a very prominent posterior tubercle, and its anterior tubercle is either absent or rudimentary.¹¹ The unique sonomorphology of the C7 TP was used as the key anatomic landmark,¹¹ to identify the individual neural elements of the BP in the recorded sonograms. The ventral ramus of C7 is typically located on the anterior surface of the C7 TP (figure 2). Color or Power Doppler ultrasound was also used to visualize the vertebral artery and to differentiate it from the C7 ventral ramus (Fig. 3, online

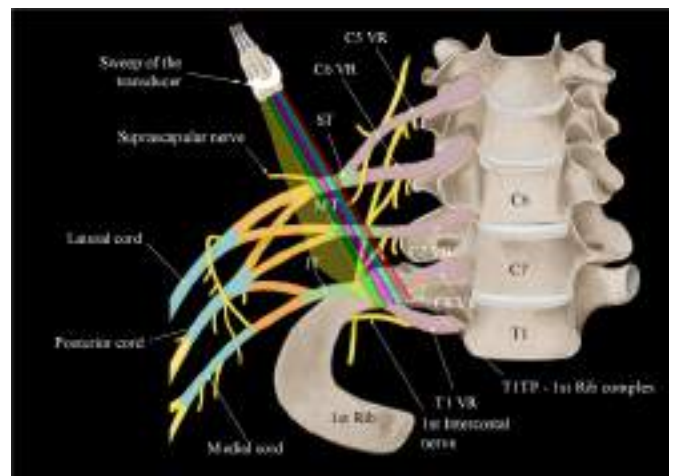


Figure 8 Illustration showing how the ultrasound transducer is angled and swept caudally during the transverse oblique scan at the base of the neck to visualize the C8 and T1 ventral rami and their fusion to form the inferior trunk. Note how the T1 ventral ramus emerges from under the first rib and joins the C8 ventral ramus more anteriorly and on top of the first rib. Also note the position of the C8 ventral ramus relative to the T1 transverse process and first rib complex. Each individual colored pane in the figure represents the position of the ultrasound beam (plane) and the neural elements that are visualized in the sonogram at each level. IT, inferior trunk; MT, medial trunk; ST, superior trunk; TP, transverse process; VR, ventral ramus.

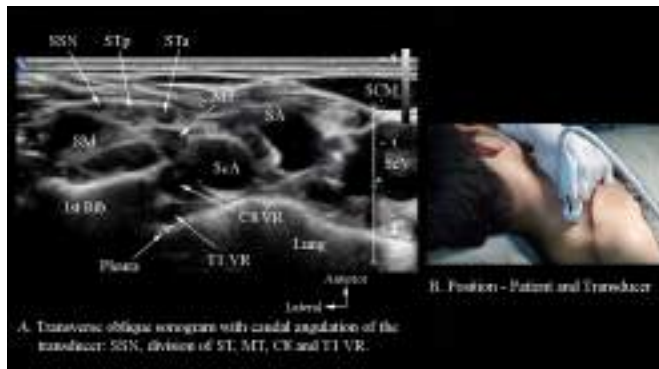


Figure 9 (A) Transverse oblique sonogram of the base of neck showing the T1 ventral ramus emerging from under the first rib and coming to lie next to the C8 ventral ramus. (B) Position of patient and ultrasound transducer during the scan. MT, middle trunk; SA, scalenus anterior muscle; ScA, subclavian artery; SCM, sternocleidomastoid muscle; ScV, subclavian vein; SM, scalenus medius muscle; SSN, suprascapular nerve; STa, anterior division of superior trunk; STp, posterior division of superior trunk; VR, ventral ramus.

supplementary digital content 2). *Step III*: the transducer was then slowly swept further cephalad, but maintaining the same orientation as in step 2 (transverse oblique), until the large C6 TP with its characteristic prominent anterior (carotid or Chassaignac) tubercle was visualized (Fig. 4, online supplementary digital content 3).¹¹ The C6 ventral ramus is located between the anterior and posterior tubercles of the C6 TP (figure 4). The C6 ventral ramus was traced back and forth to identify any sonographic evidence of intraneural septation or splitting (Figure 2, online supplementary digital content 4).^{4 10 12} *Step IV*: from the above position, the ultrasound transducer was manipulated further cephalad, maintaining the same transverse oblique orientation, until the much smaller C5 TP with its hyperechoic anterior and posterior tubercles were delineated (figure 5). The much smaller C5 ventral ramus is visualized between the two tubercles of the C5 TP (Fig. 5, online supplementary digital content 4). *Step V*: from the level of the C5 TP, the ultrasound transducer was slowly manipulated in the reverse direction, that is, caudally towards the C6 TP (figure 4). During this maneuver, attention was focused on the C5 ventral ramus¹⁰ and it was closely tracked caudally until it was seen to fuse with the C6 ventral ramus to form the superior (upper, C5–C6) trunk^{10 17 18} (Fig. 6, online supplementary digital content 5). The two round to oval hypoechoic structures located deep and caudal to the superior trunk, that is, the middle trunk (continuation of the C7 ventral ramus), and the C8 ventral ramus (located on top of the T1 TP and first rib complex),^{12 18} were then identified (Fig. 6, online supplementary digital content 5). Thereafter, the transducer was slowly swept further caudally until the origin of the suprascapular nerve and the divisions of the superior trunk into its posterior and anterior divisions were visualized^{4 20} (Fig. 7, online supplementary digital content 5). *Step VI*: identification of the branches of the superior trunk was based on the “SPA” arrangement, of the branches of the superior trunk, described by Hanna.²⁰ This refers to the sequential arrangement, from cranial and posterior to caudal and anterior, of the suprascapular nerve (S), posterior (P), and anterior (A) divisions of the superior trunk.²⁰ As the orientation of the ultrasound transducer gradually became more tilted caudally, the acoustic shadow of the neck of the first rib disappeared posteriorly and the C8 ventral ramus was seen to lie medial to the inner border of the first

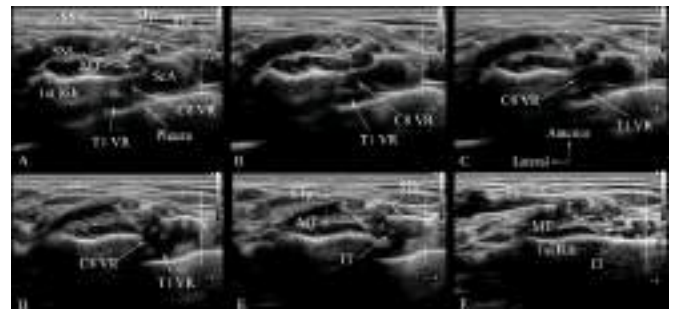


Figure 10 A sequence of transverse oblique sonograms, from a single volunteer, illustrating the formation of the inferior trunk (C8–T1). (A) T1 ventral ramus as it emerges from under the first rib, (B–E) how the T1 ventral ramus joins the C8 ventral ramus to form the inferior trunk, (F) position of the inferior trunk at the “corner pocket.” Once the T1 ventral ramus is identified, the sequence of transducer movement, to visualize the fusion of the C8 and T1 ventral rami to form the inferior trunk, involves a slow sliding back and forth sweeping motion while focusing on the T1 ventral ramus. IT, inferior trunk; MT, middle trunk; ScA, subclavian artery; SM, scalenus medius; SSN, suprascapular nerve; ST, superior trunk; STa, anterior division of superior trunk; STp, posterior division of superior trunk; VR, ventral ramus.

rib and adjacent to the dome of the pleura/lung (Fig. 7, online supplementary digital content 6). *Step VII*: from the above position, the ultrasound transducer was gently tilted further caudally with a slow sweeping motion and a gradually increasing angle (figure 8) until the T1 ventral ramus was seen to emerge from under the first rib and come to lie next and caudal to the C8 ventral ramus (Fig. 9, online supplementary digital content 6). From this position, the ultrasound transducer was manipulated with a gentle sliding back and forth sweeping motion (figure 8) to visualize the fusion of the C8 and T1 ventral rami to form the inferior (lower, C8–T1) trunk (Fig. 10, online supplementary digital content 6) and come to lie lateral to the subclavian artery on top of the first rib.²

RESULTS

Ultrasound imaging of the BP was successfully performed above the clavicle in all five volunteers (gender, three male, two female; age, 36–44 years; weight, 49–60 kg; height, 154–170 cm; body mass index, 19.2–20.8 kg/m²; and ASA, I) using the technique described above. The neural elements of the BP that were visualized in all volunteers included the ventral rami of C5–T1, the three trunks (superior, middle, and inferior), origin of the suprascapular nerve from the superior trunk, divisions of the superior trunk, and formation of the inferior trunk (C8–T1) (figures 1–12, online supplementary digital content 1–8). We were unable to delineate the divisions of the middle and inferior trunk in any of our volunteers. At the supraclavicular fossa, the neural elements were visualized as a cluster of round to oval hypoechoic structures located on the posterolateral aspect of the pulsatile subclavian artery and on top of the first rib (figure 1). The C7 ventral ramus was visualized as a round to oval hypoechoic structure lying anterior to the C7 TP and lateral to the vertebral artery (figure 2). The C5 (figure 5) and C6 (figure 4) ventral rami were also round to oval hypoechoic structures and seen to emerge between the anterior and posterior tubercles of their respective TPs. The C6 ventral ramus also exhibited echogenic internal septation with a frankly split (bifid) appearance in four of the five volunteers (Fig. 2, online supplementary digital content 7). In three of the four volunteers

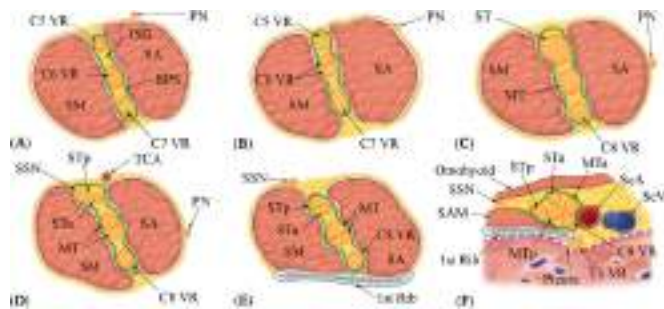


Figure 11 Illustration depicting how the elements of the brachial plexus were visualized during the ultrasound scan in this study. BPS, brachial plexus sheath; ISG, interscalene groove; IT, inferior trunk; MT, middle trunk; MTa, anterior division of the middle trunk; MTp, posterior division of the middle trunk; PN, phrenic nerve; SA, scalenus anterior; SAM, serratus anterior muscle; ScA, subclavian artery; ScV, subclavian vein; SM, scalenus medius; SSN, suprascapular nerve; ST, superior trunk; STa, anterior division of superior trunk; STp, posterior division of superior trunk; TCA, transverse cervical artery; VR, ventral ramus.

with a bifid C6, the ventral ramus of C7 was also bifid (online supplementary digital content 7). The C5 and C6 ventral rami fused to form the superior trunk (figure 5) after which it gave off the suprascapular nerve laterally and split into its posterior and anterior divisions (figure 7). The middle trunk, which is the continuation of the C7 ventral ramus, was seen lying deep to the superior trunk and within the interscalene groove (figure 6). The C8 ventral ramus was identified deep to the middle trunk and lying on top of the T1 TP and first rib complex (Fig. 6, supplementary digital content 5 and 6). The T1 ventral ramus was seen to emerge from under the first rib, initially lying inferior to the C8 ventral ramus posteriorly (figure 9), after which the C8 and T1 ventral rami fused to form the inferior (lower) trunk more anteriorly (Fig. 10, online supplementary digital content 6) and came to lie lateral to the subclavian artery at the “corner pocket” (figure 10F). We did not observe any internal septation or splitting of the C8 and T1 ventral ramus. The interscalene groove was partitioned by invagination of the scalenus anterior muscle between the C5 and C6 ventral rami (in two of five volunteers),

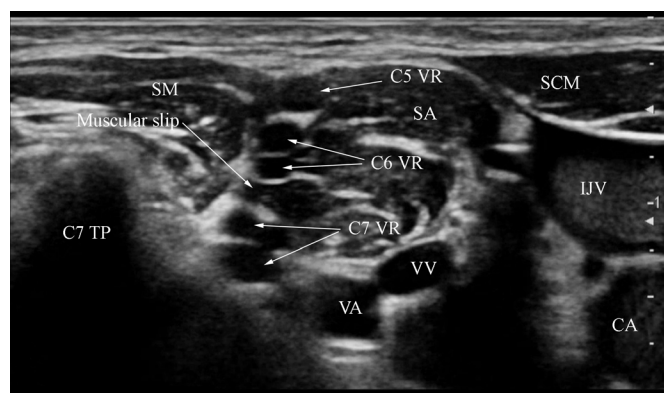


Figure 12 Transverse oblique sonogram at the level of the C7 transverse process demonstrating internal septation and splitting of the C6 and C7 ventral rami. Also note the thick muscular slip separating the C6 and C7 ventral rami and connecting the scalenus anterior and medius muscle. CA, carotid artery; IJV, internal jugular vein; SA, scalenus anterior muscle; SCM, sternocleidomastoid muscle; SM, scalenus medius muscle; VA, vertebral artery; VR, ventral ramus; VV, vertebral vein; TP, transverse process.

or by muscular slips between the scalenus anterior and medius muscles (online supplementary digital content 8). The latter was also seen to separate the C6 and C7 ventral rami (in four of five volunteers), or the middle trunk and C8 ventral ramus (in one of five volunteers).

DISCUSSION

This study aimed to evaluate a high definition ultrasound imaging technique, using scan planes typically used during USG BPB,^{2,8} to systematically identify the individual elements of the BP above the clavicle. Using the scan sequence described, we were able to identify the C5–T1 ventral rami, the three trunks (superior, middle, and inferior), divisions of the superior trunk and formation of the inferior trunk (C8–T1) in all five volunteers. Currently, there are numerous reports of ultrasound imaging of the BP,^{2,3,5,7,9,11,12,18} but we believe this is the first report to comprehensively demonstrate majority of the main components of the BP above the clavicle including the T1 ventral ramus and formation of the inferior trunk (C8–T1).

Being able to visualize the C5–T1 ventral rami in all volunteers is in agreement with published data demonstrating that it is feasible to sonographically identify the C5–C8 ventral rami in majority (C5–C7 in 100% and C8 in 80%–100%)^{11,18,19} of individuals using a transverse oblique scan,^{11,18,19} but contradicts assertions that it is not feasible to image the T1 ventral ramus because of its deep location,^{5,9} interposition of the neck of the first rib over the T1 intervertebral foramen,⁹ and limited transducer access.⁵ In this study, the T1 ventral ramus was visualized using a transverse oblique scan with a caudally angled (approximately 30–40°) transducer (Fig. 9, online supplementary digital content 6).¹¹ We believe the caudal angulation overcomes the acoustic shadow of the neck of the first rib by aligning the ultrasound beam with the T1 ventral ramus after it has emerged from underneath the neck of the first rib (figure 8). Accurate identification of the individual ventral rami is desirable because it allows accurate injection of the C5 and C6 ventral ramus during an interscalene BPB, or selectively perform a superior trunk block,¹⁷ for shoulder surgery. Furthermore, targeted injections of the T1 ventral ramus and/or the inferior trunk (C8–T1) may circumvent inferior trunk or ulnar nerve sparing during an interscalene²¹ or supraclavicular²² BPB. Future research to evaluate the safety and efficacy of such targeted injection of the T1 ventral ramus and/or the inferior trunk is warranted.

The septation and splitting (bifid appearance) of the C6 and C7 ventral rami that we observed is in agreement with previous reports^{4,10,12} and confirms the multifascicular (two to seven fascicles per ventral rami) internal architecture of these nerves.²³ Our finding also supports previous claims that all hypoechoic nodules within the interscalene groove does not represent a single ventral ramus.¹⁵ Therefore, the “stoplight sign”⁴ may only represent two nerves (C5–C6–C6).^{4,15} We also concur with Franco and Williams’s⁴ that an injection between the two fascicular bundles of the bifid C6 ventral ramus, during an interscalene BPB, may represent an intraneural injection. Furthermore, if both the C6 and C7 ventral rami are bifid, as in some of our volunteers (Fig. 12, online supplementary digital content 7), then the five elements of the BP that are stacked one on the other within the interscalene groove represents only three nerves (C5–C6–C6–C7–C7) and not all the five ventral rami (C5–T1) of the BP. Observations like these underscore the clinical importance of performing a systematic ultrasound examination of the BP before an interscalene BPB. Since there are potential safety issues with interscalene BPB in patients with a split C6 ventral

ramus, it may be prudent to perform the less aggressive “perplexus” injection technique than the more-aggressive “intra-perplexus” injection technique for interscalene BPB²⁴ since the resultant block dynamics are comparable.²⁴

The most common arrangement of the three trunks within the interscalene groove in our volunteers, in a cranial to caudal direction, was the superior trunk-middle trunk-C8 ventral ramus with the latter lying on top of the T1 TP and first rib complex (figures 6 and 11).¹⁸ The inferior trunk was always identified distal to the C8 ventral ramus and at the “corner pocket” of the supraclavicular fossa (figure 10). Accurate identification of all three trunks of the BP may allow selective injection of these nerves to produce surgical anesthesia of the entire upper extremity, except for the intercostobrachial nerve (T2) territory, which is otherwise not possible with any single BPB technique in use today. Previous researches have addressed this dilemma using a combination of BPB techniques^{25 26} but with relatively large volumes of local anesthetics (40–50 mL). Our preliminary experience with USG “selective trunk block,” for surgical anesthesia of the entire upper extremity, and using smaller volumes of local anesthetic (25 mL) has been very encouraging and our results will be reported shortly.

The suprascapular nerve emerged from the lateral aspect of the superior trunk after which the superior trunk split into its two divisions. Being able to accurately identify the superior trunk and the suprascapular nerve is encouraging because selective “superior trunk block”¹⁷ and “anterior suprascapular nerve block”¹⁶ are non-inferior,^{16 17} but phrenic nerve sparing,¹⁷ alternatives to interscalene BPB for postoperative analgesia after shoulder surgery. There is controversy about the anatomical arrangement of the two divisions of the superior trunk. Most standard anatomy textbooks and published literature depict the branches and divisions of the superior trunk in the following order from cranial to caudal: suprascapular nerve, anterior division, and posterior division (figure 8).^{5 7 9} However, recent research in cadavers^{4 20} has shown that they are consistently arranged as suprascapular nerve, posterior division, and anterior division^{4 20} and hence the acronym “SPA.”²⁰ One may argue that it is a matter of semantics for anesthesiologists as to which of the two division of the superior trunk in the sonogram is the anterior or posterior division since we rarely attempt to block them individually or selectively. However, Hanna²⁰ discusses that it is imperative for surgeons performing neurotization (nerve transfer) surgery to correctly identify these divisions since these three nerves are frequent targets for BP repair.²⁰ Therefore, future studies to accurately characterize the trifurcation of the superior trunk in the clinical setting is warranted.

Partitioning of the interscalene groove by scalene muscle slips (bridges), as seen in this report, is rarely reported in the anesthetic literature.^{14 27} However, a review of the literature indicates that scalene muscle anomalies, such as the scalenus minimus muscle²⁸ or interconnecting muscular slips between the scalenus medius and scalenus anterior muscles²⁹ are not uncommon.²⁸ The muscular slip visualized between the C6 and C7 ventral rami is most probably one of the interconnecting muscular slips between the scalenus medius and scalenus anterior muscle.^{28 29} Based on the location of the muscular slip between the middle trunk and C8 ventral ramus (figure 6), and the anatomy of the scalenus minimus muscle,²⁸ we believe it is this muscle.²⁸ Partitioning of the lower part of the interscalene groove by scalene muscle slips may restrict the caudal spread of local anesthetic after an interscalene BPB and may explain why it fails to anesthetize the forearm and hand.³⁰ Future research should characterize in detail the muscular slips between the scalene muscles

and evaluate their effect on block dynamics after an interscalene BPB.

Our study has several limitations. It was not randomized, had a small sample size, and subjects were young with low body mass index. We did not randomize our volunteers because this study aimed to evaluate a high definition ultrasound imaging technique to identify the individual elements of the BP above the clavicle. The body mass index of our volunteers was low but is consistent with the body habitus of the population at the investigators institute. We excluded volunteers who were obese or had a short neck because ultrasound imaging of the BP in these subjects is challenging.¹⁸ Therefore, our results may not apply to the elderly, obese, and those with a short neck and future research in these subjects is warranted. No alternate imaging technique was used to confirm the identify of the neural elements of the BP in this study but was based on a validated¹¹ and well-accepted method^{12 18 19} of using the unique sonomorphology of the C7 TP.¹¹ Future research should evaluate the reliability and reproducibility of the ultrasound scan technique described in this report in a larger and more heterogeneous group of subjects.

In conclusion, using high definition ultrasound imaging, we were able to systematically identify majority of the main components of the BP above the clavicle, with the exception of the divisions of the middle and inferior trunk. Future research should evaluate how the new information from this study can be used to refine existing BPB techniques and develop novel upper extremity blocks.

Contributors MKK was involved with conception, planning and design of study, conduct of study, acquisition of data, review of data, data interpretation, and reporting/preparation of manuscript. JP was involved with planning and design of the study, conduct of study, acquisition of data, review of data, data interpretation, and preparation of manuscript. BS and AP were involved with conduct of study, acquisition of data, review of data, data interpretation, and review of manuscript.

Funding This work was locally funded by the Department of Anaesthesia and Intensive Care, The Chinese University of Hong Kong, Prince of Wales Hospital, Shatin, Hong Kong, China.

Competing interests None declared.

Patient consent for publication Not required.

Ethics approval This prospective, observational study was approved by The Joint Chinese University of Hong Kong—New Territories East Cluster Clinical Research Ethics Committee.

Provenance and peer review Not commissioned; externally peer reviewed.

Data availability statement Data sharing not applicable as no data sets generated and/or analyzed for this study. Prospective observational study so no data sets generated.

ORCID iD

Manoj Kumar Karmakar <http://orcid.org/0000-0002-3674-2095>

REFERENCES

- Chan VWS. Applying ultrasound imaging to interscalene brachial plexus block. *Reg Anesth Pain Med* 2003;28:340–3.
- Perlas A, Chan VWS, Simons M. Brachial plexus examination and localization using ultrasound and electrical stimulation. *Anesthesiology* 2003;99:429–35.
- Sheppard DG, Iyer RB, Fenstermacher MJ. Brachial plexus: demonstration at US. *Radiology* 1998;208:402–6.
- Franco CD, Williams JM. Ultrasound-guided interscalene block: Reevaluation of the “stoplight” sign and clinical implications. *Reg Anesth Pain Med* 2016;41:452–9.
- Griffith JF. Ultrasound of the brachial plexus. *Semin Musculoskelet Radiol* 2018;22:323–33.
- Kapral S, Greher M, Huber G, et al. Ultrasonographic guidance improves the success rate of interscalene brachial plexus blockade. *Reg Anesth Pain Med* 2008;33:253–8.
- Lapegue F, Faruch-Bilfeld M, Demondion X, et al. Ultrasonography of the brachial plexus, normal appearance and practical applications. *Diagn Interv Imaging* 2014;95:259–75.
- Orebaugh SL, McFadden K, Skorupan H, et al. Subepineurial injection in ultrasound-guided interscalene needle tip placement. *Reg Anesth Pain Med* 2010;35:450–4.

- 9 Martinoli C, Gandolfo N, Perez MM, *et al.* Brachial plexus and nerves about the shoulder. *Semin Musculoskelet Radiol* 2010;14:523–46.
- 10 Filip P. Complex arithmetic at the brachial plexus roots. *Reg Anesth Pain Med* 2009;34:79–80.
- 11 Martinoli C, Bianchi S, Santacroce E, *et al.* Brachial plexus sonography: a technique for assessing the root level. *Am J Roentgenol* 2002;179:699–702.
- 12 Haun DW, Cho JCS, Kettner NW. Normative cross-sectional area of the c5-c8 nerve roots using ultrasonography. *Ultrasound Med Biol* 2010;36:1422–30.
- 13 Kessler J, Schafhalter-Zoppoth I, Gray AT. An ultrasound study of the phrenic nerve in the posterior cervical triangle: implications for the interscalene brachial plexus block. *Reg Anesth Pain Med* 2008;33:545–50.
- 14 Soeding P, Eizenberg N. Review article: anatomical considerations for ultrasound guidance for regional anesthesia of the neck and upper limb. *Can J Anesth/J Can Anesth* 2009;56:518–33.
- 15 Grant SA, Smith EC. Ultrasound of cervical roots and brachial plexus in neonates. *Muscle Nerve* 2015;51:626.
- 16 Auyong DB, Hanson NA, Joseph RS, *et al.* Comparison of anterior Suprascapular, supraclavicular, and Interscalene nerve block approaches for major outpatient arthroscopic shoulder surgery. *Anesthesiology* 2018;129:47–57.
- 17 Kim DH, Lin Y, Beathe JC, *et al.* Superior trunk block: a phrenic-sparing alternative to the interscalene block: a randomized controlled trial. *Anesthesiology* 2019;131:521–33.
- 18 Won SJ, Kim B-J, Park KS, *et al.* Measurement of cross-sectional area of cervical roots and brachial plexus trunks. *Muscle Nerve* 2012;46:711–6.
- 19 Zhu Y-S, Mu N-N, Zheng M-J, *et al.* High-resolution ultrasonography for the diagnosis of brachial plexus root lesions. *Ultrasound Med Biol* 2014;40:1420–6.
- 20 Hanna A. The spa arrangement of the branches of the upper trunk of the brachial plexus: a correction of a longstanding misconception and a new diagram of the brachial plexus. *J Neurosurg* 2016;125:350–4.
- 21 Lanz E, Theiss D, Jankovic D. The extent of blockade following various techniques of brachial plexus block. *Anesth Analg* 1983;62:55–8.
- 22 Fredrickson MJ, Patel A, Young S, *et al.* Speed of onset of ‘corner pocket supraclavicular’ and infraclavicular ultrasound guided brachial plexus block: a randomised observer-blinded comparison. *Anaesthesia* 2009;64:738–44.
- 23 Bonnel F. Microscopic anatomy of the adult human brachial plexus: an anatomical and histological basis for microsurgery. *Microsurgery* 1984;5:107–17.
- 24 Spence BC, Beach ML, Gallagher JD, *et al.* Ultrasound-Guided interscalene blocks: understanding where to inject the local anaesthetic. *Anaesthesia* 2011;66:509–14.
- 25 Brown AR, Parker GC. The Use of a “Reverse” Axis (Axillary-Interscalene) Block in a Patient Presenting with Fractures of the Left Shoulder and Elbow. *Anesth Analg* 2001;93:1618–20.
- 26 Guttman OT, Soffer RJ, Rosenblatt MA. The ultrasound-guided supraclavicular-interscalene (ugscis) block: a case report. *Pain Pract* 2008;8:62–4.
- 27 Kessler J, Gray AT. Sonography of scalene muscle anomalies for brachial plexus block. *Reg Anesth Pain Med* 2007;32:172–3.
- 28 Harry WG, Bennett JDC, Guha SC. Scalene muscles and the brachial plexus: anatomical variations and their clinical significance. *Clin. Anat.* 1997;10:250–2.
- 29 Yamamoto C. Typological interrelationships of the human scalenus muscles, brachial plexus and subclavian artery. *Okayama Igakkai Zasshi* 1992;104:205–19.
- 30 Madison SJ, Humsi J, Loland VJ, *et al.* Ultrasound-guided root/trunk (interscalene) block for hand and forearm anesthesia. *Reg Anesth Pain Med* 2013;38:226–32.